A Coil with Distributed Capacitance Elements For Microimaging at 3 T

J. Lazovic[1], C. M. Collins[2], M. B. Smith[2]

[1]Molecular Medicine, Penn State College of Medicine, Hershey, PA, United States, [2]Radiology, Penn State College of Medicine, Hershey, PA, United States

INTRODUCTION: In high field imaging distributed capacitors are used to achieve self-resonance in electrically long structures and achieve the small capacitances necessary for resonance at these high frequencies with large coils [1, 2]. In smaller coils, where coil noise is dominant, use of distributed capacitance may reduce loss associated with lumped element capacitors. Birdcage radiofrequency (RF) coils are preferred for applications where excellent RF magnetic (B_1) field homogeneity is required. Slotted-tube resonators are often preferable for applications where high SNR is required, and where excellent B_1 field homogeneity is not critical. Since better SNR is always desirable the goal of the current design was to achieve good homogeneity of the birdcage coil and improve SNR by using the distributed capacitance approach. While design of the slotted tube resonator is limited to a linear mode of transmission and reception, the described coil design can be driven in quadrature.

METHODS: An 8 element distributed capacitance coil was constructed on a Teflon cylinder with dimensions of 2.2 cm OD, 2.1 cm ID, 3.5 cm length and 4 mm leg width. The coil consisted of 8 pairs of legs, where each pair has one leg placed on the outside surface of the Teflon cylinder and the other leg placed on the inside surface of the Teflon cylinder thus serving as a distributed capacitor (4 pF) with Teflon being the dielectric material. There are two end-rings, one on each end of the coil, one placed on the outside surface and other placed on the inside surface of Teflon cylinder. A schematic diagram of the coil is shown in Fig. 1A. The resonant frequency of this arrangement was ~163 MHz. In order to achieve ~125 MHz frequency, additional 20 pF capacitors were placed on the end-rings elements in the form of lumped element capacitors, Fig 1B. Alternative methods to lower the resonant frequency would be to reduce the thickness of the dielectric material, or to simply use substrate with a higher dielectric constant. For SNR comparison a slotted tube resonator was made to match the OD and length of the distributed capacitance coil. MR imaging was performed on a 3.0 T MRI spectrometer (Medspec S300, Bruker Instruments, Ettlingen, Germany) with a small aperture gradient coil (9.5 cm aperture and 1.1 T/m gradient strength). A three month old mouse and 50 mM saline phantom (1.7 cm diameter) were imaged in two coils using a T_2-weighted spin echo sequence (TR/TE=3000/10.13-151.95 ms, 256 X 128 matrix size, field of view 2 x 2 cm^2, N=15 echoes, NEX=2 (NEX=1 for the saline phantom), 10 slices, 0.5 mm slice thickness in 13 min). In addition, B_1 field homogeneity was evaluated using the signal intensity ratio of 45^0 and 90^0 flip angle gradient echo images (TR/TE=500/6 ms, 256 X 256 matrix and 4 X 4 cm field of view, 4 mm slice thickness) with 1.7 cm diameter 50 mM saline phantom and a previously described procedure [3]. The coil with distributed capacitance elements with end capacitors, Fig.1 B, and the lumped-element low-pass birdcage coil (same length, 8 elements, 4 mm leg width) were modeled with the FDTD method (1 mm cell size) and the models were tuned to 125 MHz and driven with a 1 V source at one location.

RESULTS: The coil was tuned to 125.44 MHz for proton imaging at 3 T, and had ~8 MHz tuning range. RF power requirements to achieve 90^0 flip angle were ~2 dB lower for the distributed capacitance coil when compared to the slotted tube resonator. The described coil had ~30% better SNR compared to the slotted tube resonator, for both the saline phantom and the mouse brain. A mouse brain image acquired with the distributed capacitance elements coil is shown in Fig. 2. The experimental B_1 field map for the distributed capacitance showed that the B_1 filed distribution across the coil is within 10^0 flip angle for the saline phantom, which is comparable to a low-pass birdcage coil with similar dimensions. In the FDTD simulations, the field at the center of the distributed capacitor element coil was approximately 45% higher than that in the lumped-element low-pass birdcage coil when both models were driven with identical voltages, Fig. 3. Assuming the coil noise dominance, based on the B_1 field calculations, we predict described coil to have 45% better SNR than the lumped-element low-pass birdcage coil.

DISCUSSION: A novel coil for microimaging at 3 T is presented. Both goals for high SNR and good B_1 field homogeneity are achieved. The distributed capacitance coil has very little coupling with the surroundings and the B_1 field is well contained, so the coil was found not to need an RF shield. A further improvement in SNR is possible by driving the coil in quadrature. A further improvement in the B_1 field homogeneity can be achieved using 16 leg pairs instead of the proposed 8 pairs. The distributed capacitance coil design can be easily implemented for other magnetic field strengths by varying the thickness of the dielectric material or choosing material with a different dielectric constant.

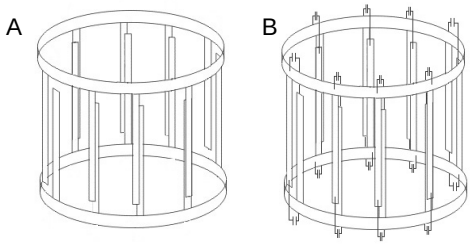

Figure 1. Schematics of the distributed capacitance coil. (A) the original design, and (B) with the additional 20 pF capacitors. The dielectric material is placed between the inner and outer coil segments. Tuning and matching network can be placed across any leg element.

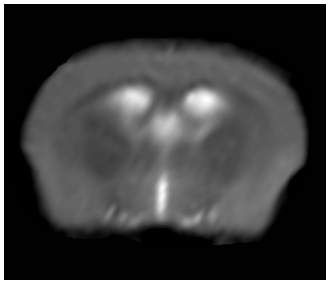

Figure 2. Representative T2-weighted coronal slice of the mouse brain acquired with the distributed capacitance coil and spin echo sequence (TR/TE=3000/10 –150 ms).

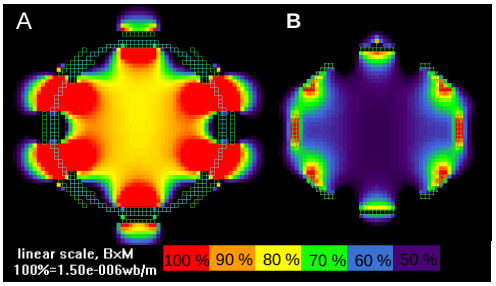

Figure 3. Calculated B_1 field distribution for the coil with distributed capacitance elements (A) and lumped-element low-pass birdcage coil (B). Both coils are shown scaled to the same maximal B_1 field value. The scale is given in the percentage of B_1 field magnitude.

ACKNOWLEDGMENTS: This work was supported by HD 30705 to MBS.

REFERENCES:

1. Vaughan JT et al. Magn Reson Med 1994; 32:206-18.
2. Zhang X et al. J Magn Reson 2003; 161:242-51.
3. Insko EK and Bolinger L. JMRa, 103:82-85, 1993.